Surface-Modified Superparamagnetic Iron-Oxide Nanoparticles

Wolfgang H. Binder[*] and **Harald C. Weinstabl**

Martin-Luther Universität Halle-Wittenberg, Lehrstuhl Makromolekulare Chemie, Institut f. Chemie, Halle, Germany

Summary. The generation of superparamagnetic iron-oxide nanoparticles bearing fluorescent ligands is described. γ-Fe$_2$O$_3$ nanoparticles (radius $\sim$4 and 8 nm) bearing octylamine or oleic acid as ligands were prepared by hydrothermal synthesis starting from Fe-cupferron and iron pentacarbonyl, respectively. Ligand exchange proceeds with 1,2-diols bearing ω-azido or ω-bromo ligands at elevated temperatures. Subsequent nucleophilic substitution reaction, followed by 1,3-dipolar cycloaddition reactions with 2,4,6-trinitro-1-O-propargyl-benzene yields superparamagnetic iron-oxide nanoparticles with a fluorescent ligand on their surface.

Keywords. Iron oxide nanoparticles; 1,3-Dipolar cycloaddition-reactions; Superparamagnetism; Surface-modification.

Introduction

Superparamagnetic nanoparticles are of growing interest within the last decade of scientific research. Due to their superparamagnetic nature at room temperature, they have far-ranging applications in material and medicinal science. These properties are provided by many different elemental compositions, such as Ni, Co, Co–Cu, Co–Pt, Co–Pd, Fe–Pt, Fe–Pd, Fe$_3$O$_4$, and γ-Fe$_2$O$_3$ [1–4]. In practice, especially in medicinal science, augmented superparamagnetic iron-oxide nanoparticles (SPIONs) are used due to their accessibility as well as their non-toxic and highly biocompatible character. In order to direct recognition processes in living systems, surface-modification of the inorganic nanoparticle core

with a suitable and functional organic core represents an important issue in nanoparticle research. In the case of superparamagnetic iron-oxide nanoparticles a plethora of different methods, mostly relying on ligand exchange reactions has been reported, enabling the modification with polymeric [5], organic [6], inorganic [7], and peptidic ligands [8].

Presently we are interested in the surface modification of nanoparticles with functional organic ligands in order to enable the assembly of the thus functionalized nanoparticles on polymers [9], into bulk-materials [10], or surfaces [11]. An important synthetic methodology thereto is based on the azide/alkine-"click"-reaction (also known as the *Sharpless-Huisgen* "click"-reactions) [12]. In the present publication, we report on the modification of γ-Fe$_2$O$_3$-nanoparticle-surfaces by use of the azide/alkine-"click" reaction relying on an initial ligand exchange reaction (see Fig. 1), followed by a subsequent dipolar cycloaddition reaction with a fluorescent ligand, thus leading to the attachment of the fluorescent ligand onto the nanoparticle surface.

Synthesis of Superparamagnetic Nanoparticles

The basic strategy for the preparation of surface modified γ-Fe$_2$O$_3$ nanoparticles is shown in Scheme 1. Thus nanoparticles (**NP1** or **NP2**) are reacted with a suitable 1,2-diol-ligand **1a** or **1b** bearing the appropriate terminal azide- or bromo-moiety at the respective chain end. γ-Fe$_2$O$_3$ nanoparticles (SPIONs) were prepared *via* two different synthetic routes,

* Corresponding author. E-mail: wolfgang.binder@chemie.uni-halle.de

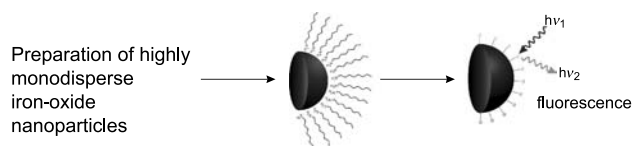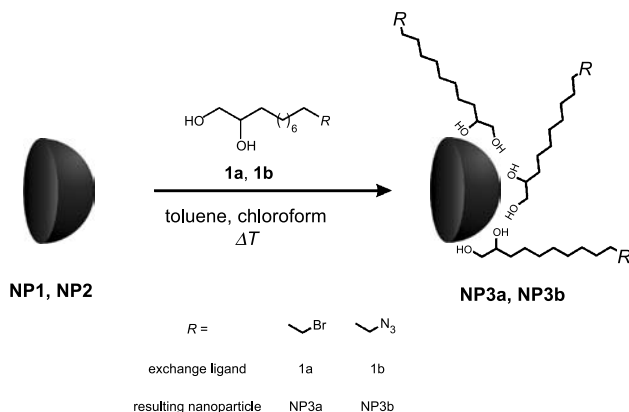**Fig. 1.** General approach for the modification of iron-oxide nanoparticles with fluorescent ligands

Scheme 1. Approach towards functionalized nanoparticles *via* ligand exchange using 1,2-diol-ligands **1a** and **1b**
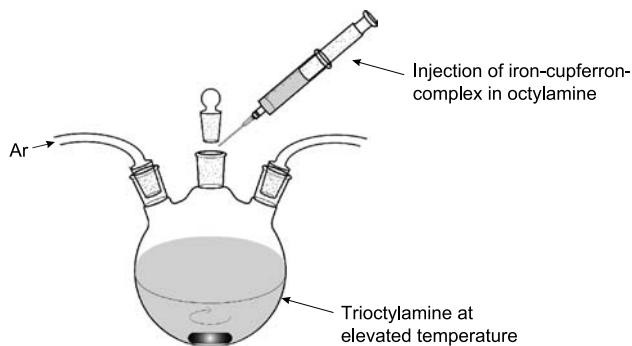

Fig. 2. Solvothermal method for the preparation of superparamagnetic iron-oxide nanoparticles
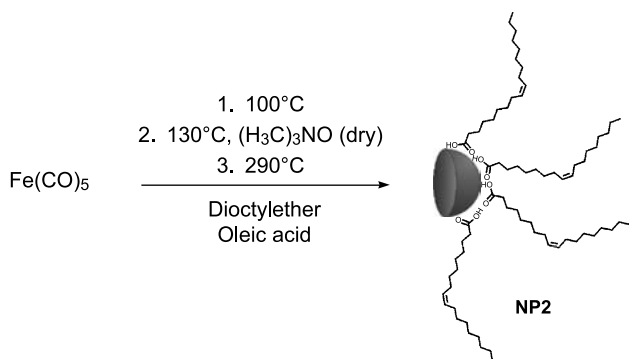

Fig. 3. Preparation of oleic acid coated iron-oxide nanoparticles *via* decomposition of iron pentacarbonyl

both relying on hydrothermal decomposition of appropriate organic iron-precursor molecules (see Fig. 2). The first route, based on *Alivisatos et al.* [13], generates monodisperse octylamine covered iron-oxide nanoparticles with a diameter of ∼8 nm. The second synthetic route (see Fig. 3) according to *Hyeon et al.* [14] resulted in highly monodisperse oleic acid covered iron-oxide nanoparticles with a diameter of ∼16 nm. Both types of nanoparticles

Table 1. Size (hydrodynamic radius) of the prepared iron-oxide nanoparticles

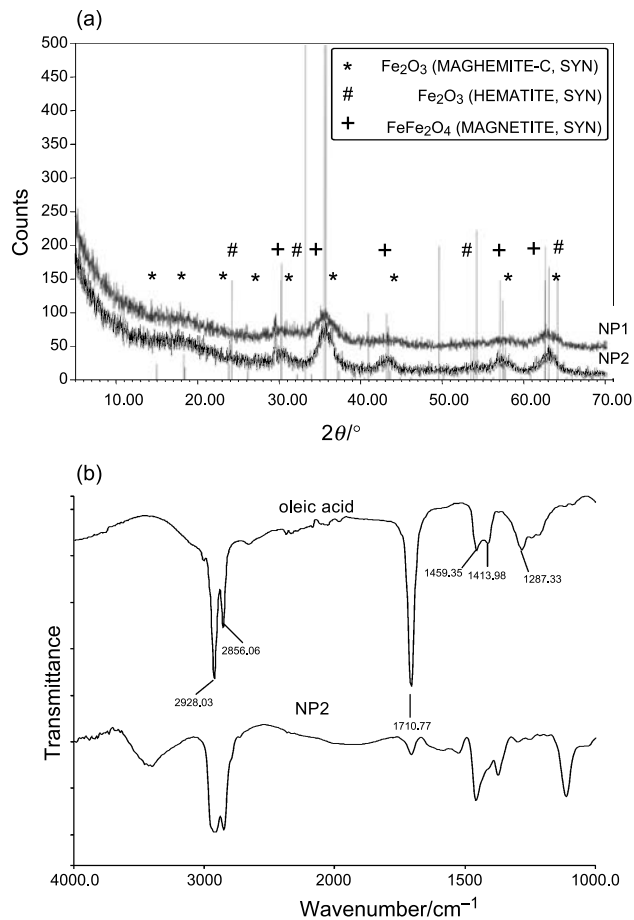| Nanoparticle batch	Hydrodynamic radius (r_h)
NP1a	3.92 nm
NP1b	3.59 nm
NP2	8.00 nm

Fig. 4. (a) XRD spectrum of **NP1** and **NP2**, proving the presence of *maghemite C* crystal structure. (b) FTIR spectrum of oleic acid functionalized nanoparticles (**NP2**). Top: spectrum of pure oleic acid, bottom: oleic acid functionalized nanoparticles

are stable in solution over months, as judged by dynamic light scattering measurements (DLS) (see Table 1). Thus, the size of the nanoparticles remains within the limit observed in the literature [13].

XRD measurements were performed to determine the crystal lattice of the synthesized SPIONs (see Fig. 4a). The obtained reflexes fit perfectly to the reflection pattern of γ-Fe$_2$O$_3$, thus proving the expected modification. Due to the small size of the nanoparticle in comparison the bulk material, the reflexes are not as sharp but the angle-2Θ-values fit to the bulk pattern. The characterization of the nanoparticles by FTIR was used to determine the surface bound ligands. Figure 4b shows the spectrum of pure oleic acid (top) and the spectrum of the nanoparticles (bottom). Characteristic peaks, such as the carbonyl band at $1710\,cm^{-1}$ can be seen proving the presence of this stabilizing ligand on the nanoparticle surface. For the evaluation of the number of surface bound ligands, TGA (Fig. 5a) measurements were performed. Additionally, the theoretical number of bound ligands was calculated (for a graphical description see Fig. 5b). As already mentioned, γ-Fe$_2$O$_3$ crystallizes in a cubic-closed-packed structure. Referring to DLS measurements the nanoparticles with an average radius of 8 nm, lead to a
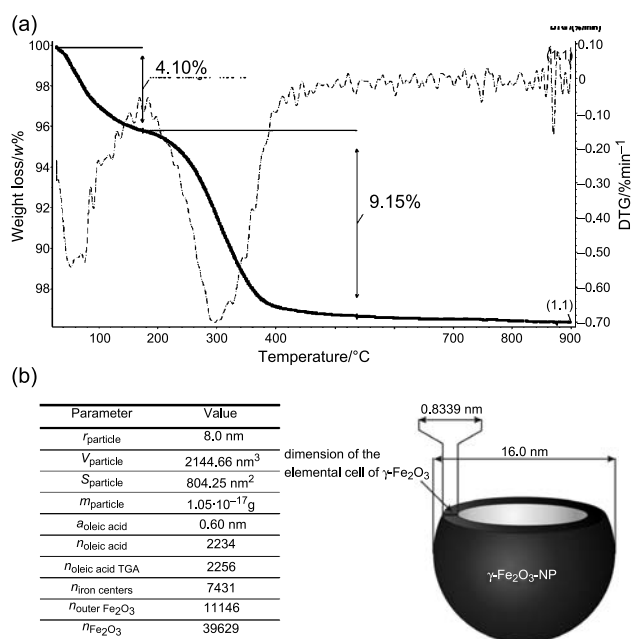
volume of the particle of $V_{particle} = 2144.66\,nm^3$ and a particle surface of $S_{particle} = 804.25\,nm^2$. Considering the density of γ-Fe$_2$O$_3$ ($\rho_{Fe_2O_3} = 4.9\,gcm^{-3}$) [15] the theoretical mass of one particle ($m_{particle}$) can be calculated as $1.05 \cdot 10^{-17}$ g. Taking the surface of one particle ($S_{particle}$) and the binding area of one ligand ($A_{octylamine}$) on the nanoparticle surface into account, the amount of surface bound ligands ($n_{oleic\ acid}$) can be calculated. The binding area of one ligand is assumed as quadratic, therefore $A_{oleic\ acid} = (a_{oleic\ acid})^2$, where $a_{oleic\ acid}$ is the side length of the quadratic binding area of one ligand. Using the molecular weight of the surface bound ligand ($M_{oleic\ acid} = 282.47\,gmol^{-1}$) it is now possible to determine the theoretical mass fraction of the surface bound ligands with respect to the total mass of the nanoparticle. Furthermore, paying attention to the molar mass of γ-Fe$_2$O$_3$ ($M_{Fe_2O_3} = 159.7\,gmol^{-1}$) and to the length of the elemental cell of γ-Fe$_2$O$_3$ ($a_{Fe_2O_3} = 0.8339\,nm$) it is possible to determine the number of γ-Fe$_2$O$_3$-units per nanoparticle ($n_{Fe_2O_3}$) and in the outer shell of the nanoparticle ($n_{outer\ Fe_2O_3}$). The calculated fraction of surface bound ligands ($9.07\,wt\%$) is in excellent agreement to TGA results ($9.15\,wt\%$) referring to the radius gained by DLS and TEM measurements. Summarized, the results indicate that the nanoparticles consist of $91\,wt\%$ iron-oxide core and $9\,wt\%$ oleic acid stabilizing ligand.

Surface-Modification of Superparamagnetic Nanoparticles

As binding site onto the nanoparticle-surface, a 1,2-diol moiety was chosen, prepared *via* a nonstereoselective *Sharpless dihydroxylation* [16]. The accretion

(a)

(b)

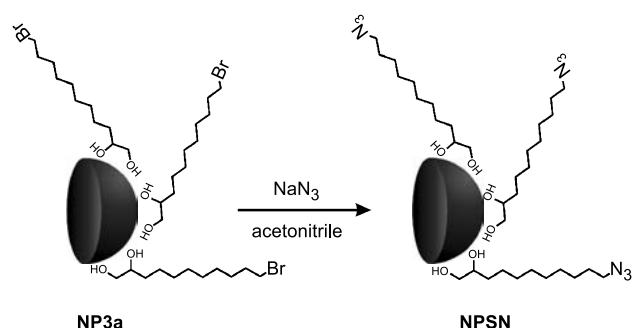| Parameter	Value
$r_{particle}$	8.0 nm
$V_{particle}$	2144.66 nm^3
$S_{particle}$	804.25 nm^2
$m_{particle}$	$1.05 \cdot 10^{-17}$ g
$a_{oleic\ acid}$	0.60 nm
$n_{oleic\ acid}$	2234
$n_{oleic\ acid\ TGA}$	2256
$n_{iron\ centers}$	7431
$n_{outer\ Fe_2O_3}$	11146
$n_{Fe_2O_3}$	39629

Fig. 5. (a) TGA of oleic acid functionalized nanoparticles **NP2**. (b) Schematic drawing and parameters for the calculation of the theoretical coverage of **NP2** with organic ligand (oleic acid)

Scheme 2. Direct nucleophilic substitution of the terminal bromine-moieties furnishing the azido-substituted nanoparticles **NPSN**

of functional azido- and bromine-groups onto the nanoparticle surface (Scheme 1) was achieved by ligand exchange reactions using the diol-ligands **1a**
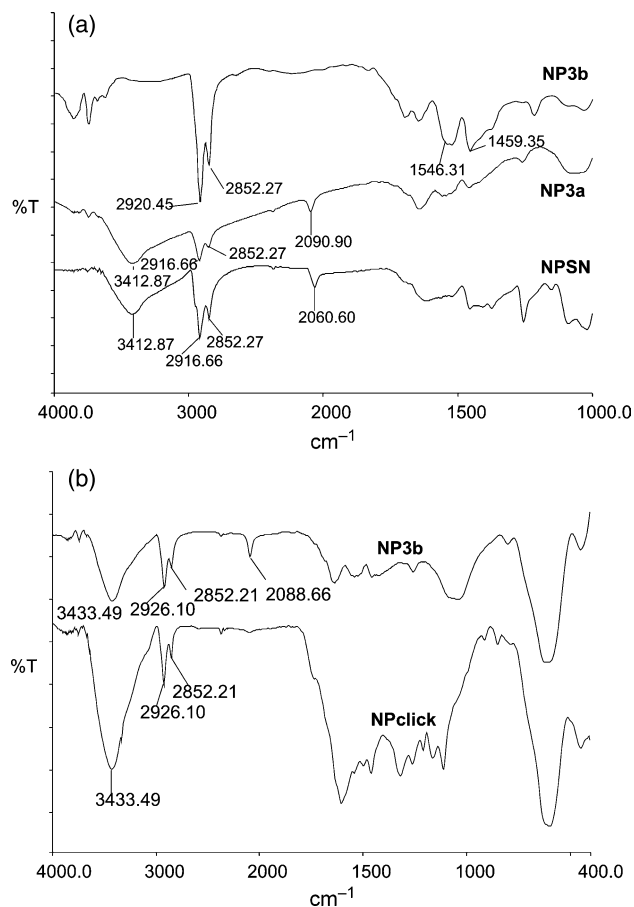

(a)

(b)

Fig. 6. (a) FTIR spectra of in-situ nucleophilic substitution on the surface of magnetic nanoparticles. Top: bromo-fuctionalized NPs, middle: azide functionalized NPs (**NP3b**), bottom: after completion of the reaction (**NPSN**). (b) FTIR spectra of nanoparticles before (top) and after (bottom) the 1,3-dipolar cycloaddition reaction of ligand **2**

and **1b**, according to the protocol of *Rotello et al.* [17]. Thus nanoparticles **NP3a** and **NP3b** were generated, bearing terminal bromine- and azido-moieties, respectively. Alternatively, nanoparticles **NP3a** can be transformed into the azido-modified nanoparticles **NPSN** *via* nucleophilic substitution reaction, as demonstrated in Scheme 2. Thus **NP3a** were suspended in acetonitrile and reacted at elevated temperatures (110°C) with sodium azide, which was suspended in the reaction mixture for 1.5 days. The resulting modified nanoparticles were precipitated by the addition of anhydrous methanol, centrifuged, and redissolved in anhydrous toluene. The starting material and the product were both analyzed by means of gravimetric methods (TGA) and IR spectroscopy (see Fig. 6a). TGA shows a weight loss of $24.91\,wt\%$ for **NP3a** and a weight loss of $21.78\,wt\%$ for **NPSN** indicating that the exchange was successfully accomplished. The IR results clearly show an appearance of the azide band at $2060\,cm^{-1}$, which is another indication for the successful nucleophilic substitution.

Finally, the thermally induced *Huisgen*-cycloaddition was investigated for the modification of the iron-oxide nanoparticles (see Scheme 3). Since the classical "click"-protocol based on Cu(I)-ions [12], cannot be applied due to the possible reduction of Cu(I) by the iron-oxide nanoparticles, the reaction was conducted without the use Cu(I)-catalysis. Therefore, **NP3b** bearing terminal azido-moieties were dissolved in dry toluene and the corresponding alkyne **2** was added. The mixture was refluxed for 2 days. The resulting functionalized nanoparticles (**NPclick**) were precipitated by the addition of dry methanol, centrifuged, and resuspended in dry toluene.
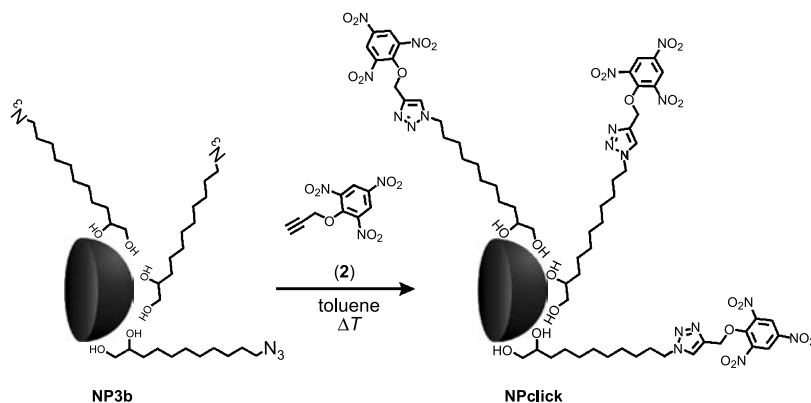
Scheme 3. 1,3-Dipolar thermal cycloaddition reaction on the surface of iron-oxide nanoparticles, affixing ligand **2** on the NP surface

This washing procedure was repeated several times in order to remove unbound ligand. Since the reaction temperature is ~110°C two reaction mechanisms are possible: one, where the ligands remain bound on the nanoparticle surface leading to a reaction directly on the nanoparticle itself, or a second mechanism, where the elevated temperature favors a detachment of the ligand, thus leading to a reaction in solution. After cycloaddition the new ligands would then rebind to the surface of the particles' surface again. The purified nanoparticles were analyzed *via* IR-spectroscopy, as shown in Fig. 6b. The disappearance of the strong azide signal at $2100 \, cm^{-1}$ and the additional appearance of the –N–O vibration at $\sim 1500 \, cm^{-1}$ indicated the successful cycloaddition performed on the nanoparticle surface.

Conclusion

We have demonstrated an approach towards the generation of $\gamma\text{-Fe}_2O_3$ nanoparticles bearing a strongly fluorescent ligand. Starting from octylamine or oleic acid modified $\gamma\text{-Fe}_2O_3$ nanoparticles, a ligand exchange reaction with 1,2-diol-ω-bromo/azido ligands was accomplished. Subsequent dipolar cycloaddition reactions furnished the fluorescently labeled $\gamma\text{-Fe}_2O_3$ nanoparticles. The method offers a generalizable approach towards differently labeled superparamagnetic iron-oxide nanoparticles. Further studies towards other functional ligands as well as their use in biomedical applications will be reported in due course.

Experimental

NMR measurements were recorded by a 200 MHz Bruker AC200 spectrometer and a 400 MHz Bruker Avance DRX 400 using CDCl$_3$ (Isotec Inc. 99.8 atom% D) and *DMSO*-d$_6$ (HDO + D$_2$O <0.02%) as solvent, at room temperature. TLC (thin layer chromatography) was performed with coated glass plates of the type Sil G-25-UV$_{254}$ obtained from the company Macherey-Nagel and TLC aluminum sheets silica gel 60 F$_{254}$ from Merck. As oxidation reagents a cerium molybate solution – "blue stain" – (1 g Ce(SO$_4$)$_2 \cdot$ 4H$_2$O, 2.5 g (NH$_4$)$_6$Mo$_7$O$_{24} \cdot$ 4H$_2$O, 6 cm^3 H$_2$SO$_4$ conc., and 90 cm^3 distilled H$_2$O) and a solution of 1 g Ce(SO$_4$)$_2 \cdot$ 4H$_2$O, 2.75 cm^3 H$_2$SO$_4$ conc., and 47 cm^3 distilled H$_2$O were used.

DLS measurements were done in toluene or *THF* solutions of the NPs after dilution by ~1/50 with pure solvent on an ALV/CGS-3 compact goniometer using the ALV-5000/E correlator software.

FTIR spectroscopy was recorded on a Biorad FTS 135 FT-IR system with a MKII Golden Gate Single Reflection ATR unit and on a Perkin Elmer System 2000 FT-IR using the software Spectrum v. 2.00 (Perkin Elmer) for data evaluation.

TEM measurements were achieved on a Phillips EM300 transmission mode 100 kV. The nanoparticle solution with a concentration of 0.1–1 mg/cm^3 in toluene was applied on standard TEM-Grids (300 mesh copper carbon only (50 ct)) purchased from Electron Microscopy Sciences.

TGA measurements were performed on a NETSCH TG 209 using synthetic air and a ceramic crucible. Data was evaluated with NETSCH Proteus – Thermal Analysis – software (V 4.3).

Preparation of Nanoparticles

Preparation of octylamine-covered nanoparticles was accomplished according to Ref. [13]. A solution of 780 mg iron cupferron (1.5 mmol) in 3.90 g of octylamine (27.22 mmol) was alternating evacuated to 10 mbar and aerated with Ar at 60°C. Trioctylamine (7.00 g, 18.33 mmol) was treated the same way at 100°C. The degassed octylamine solution was rapidly injected into the trioctylamine solution at 300°C. Immediately after the injection the reaction vessel was moved to a 225°C prewarmed bath and remained there for 30 min under vigorous magnetic stirring. After the reaction was stopped by removing the heating source, the particles were allowed to cool to room temperature. They were dissolved in anhydrous toluene, precipitated by the addition of dry methanol, centrifuged, and again dissolved in anhydrous toluene. This washing step was repeated three times. The stabilized particles were stored under Ar-atmosphere in anhydrous toluene. Particles size was determined by DLS and TEM measurements. Depending on the production batch, the size of the synthesized nanoparticles **NP1a-1d** varies between $r_h = 3.59$ nm and $r_h = 8.61$ nm (hydrodynamic radius). The stabilized NPs (**NP1**) stay soluble for several months, indicating that no agglomeration takes place. IR (KBr-pellet): $\bar{\nu} = 3450$ (–OH), 2926 (–CH$_3$, –CH$_2$–), 2857 (–CH$_3$, –CH$_2$–), 1623 (–NH$_2$), 1464 (–CH$_3$, –CH$_2$–) cm^{-1}.

Oleic acid covered iron-oxide nanoparticles were synthesized according to Ref. [14]. A mixture consisting of 0.49 cm^3 of oleic acid (1.53 mmol) and 10.7 Cm^3 dioctylether was heated to 100°C under Ar-atmosphere. Fe(CO)$_5$ (0.2 cm^3, 1.53 mmol) was injected *via* a syringe. The reaction mixture was heated to reflux (~290°C) for 1 h, whereby the color changed from orange to black. The reaction was allowed to cool to room temperature. Trimethylamine-*N*-oxide (340 mg, 4.53 mmol) was added and after addition the reaction was heated to 130°C for 2 h. The color of the reaction mixture changed from black to a brownish like color. Now the reaction was heated to reflux again. The color changed once more from brown to black again. After one hour the reaction mixture was allowed to cool to room temperature and the nanoparticles were precipitated by the addition of anhydrous ethanol. The solution was centrifuged; the precipitate was dissolved in dry toluene and again precipitated with dry ethanol. This washing step was repeated 2 more times until the nanoparticles were stored in pure anhydrous toluene. Particles size was determined by DLS measurements ($r_h = 8$ nm) and TEM measurements ($r = 7$ nm). The stabilized NPs (**NP2**) stay soluble for several months, indicating that no agglomeration takes place. IR (KBr-pellet): $\bar{\nu} = 3450$ (–OH), 2928 (–CH$_3$, –CH$_2$–), 2856

(–CH$_3$, –CH$_2$–), 1710 (C=O), 1459 (–CH$_3$, –CH$_2$–), 1414 (–COOH) cm^{-1}.

Ligand Exchange Reactions

Surface modification reactions were performed according to the general protocol for ligand exchange reactions of *Rotello et al.* [17]. All reaction steps were performed under Ar-atmosphere. Stabilized NPs (**NP1**, 50 mg) were dissolved in 30 cm^3 of a 1:1 mixture of CHCl$_3$ and toluene. A second mixture was prepared consisting of 250 mg of diol-ligand **1a** or **1b** in a 1:1-mixture of chloroform and toluene. The ligand solution was added to the nanoparticle solution *via* a syringe and the reaction mixture was heated up to 50°C under vigorous stirring for 2 days. After 48 h the exchange reaction has finished, resulting in surface modified nanoparticles **NP3a**, **3b**. Particles were purified by repeated precipitation with dry methanol, centrifugation, and resuspension in anhydrous toluene. **NP3b**: IR (KBr-pellet): $\bar{\nu} = 3420$ (–OH), 2920 (–CH$_3$, –CH$_2$–), 2848 (–CH$_3$, –CH$_2$–), 2094 (–N$_3$), 1450 (–CH$_3$, –CH$_2$–) cm^{-1}. **NP3a**: IR (KBr-pellet): $\bar{\nu} = 3420$ (–OH), 2924 (–CH$_3$, –CH$_2$–), 2857 (–CH$_3$, –CH$_2$–), 1469 (–CH$_3$, –CH$_2$–), 775 (–CH$_2$–Br) cm^{-1}.

Nucleophilic Substitution on NP3a

NP3a (50 mg) was suspended in 10 cm^3 anhydrous acetonitrile bubbled with Ar. Sodium azide (50 mg, 0.77 mmol) was added to this suspension under vigorous stirring. The reaction mixture was heated to 110°C for 1.5 days. During the reaction the precipitation of NaBr indicated gradually conversion. Solids were decanted and treated with dichloromethane. Azide functionalized nanoparticles were dissolved whereas the excess of NaN$_3$ and NaBr stayed insoluble. Particles were washed by the repeated precipitation with dry methanol, centrifugation, and redissolving in anhydrous toluene. The resulting modified nanoparticles were dried under high vacuum and analyzed by IR spectroscopy and TGA measurements. TGA showed a weight loss of 24.91 *wt*% for **NP3a** and a weight loss of 21.78 *wt*% for **NPSN** indicating that the exchange was successfully accomplished. **NPSN**: IR (KBr-pellet): $\bar{\nu} = 3412$ (–OH), 2917 (–CH$_3$, –CH$_2$–), 2852 (–CH$_3$, –CH$_2$–), 2060 (–N$_3$) cm^{-1}.

Dipolar, Thermal Cycloaddition Reactions on NP3b

NP3b (50 mg) and 100 mg 2-propargyloxy-1,3,5-trinitrobenzene (**2**, 0.40 mmol) were dissolved in anhydrous toluene. The reaction mixture was intensively bubbled with Ar and afterwards heated to 110°C for 2 days. The resulting particles were precipitated by the addition of anhydrous methanol, centrifuged, and redissolved in dry toluene. This purification cycle was repeated 3 times, until the washing solution showed no traces of 2-propargyloxy-1,3,5-trinitrobenzene (**2**). Modified particles were dried under high vacuum and analyzed with FTIR measurements as KBr-pellets. **NPclick**: IR (KBr-pellet): $\bar{\nu} = 3433$ (–OH), 2926 (–CH$_3$, –CH$_2$–), 2852 (–CH$_3$, –CH$_2$–), 1628 (O=C–NR$_2$), 1500–1600 (–NO$_2$), 1450 (–CH$_3$, –CH$_2$–) cm^{-1}.

References

[1] Fernandez CDJ, Mattei G, Maurizio C, Cattaruzza E, Padovani S, Battaglin G, Gonella F, D'Acapito F, Mazzoldi P (2005) J Magn Mater **290–291**: 187

[2] Sarkar A, Kapoor S, Yashwant G, Salunke HG, Mukherjee T (2005) J Phys Chem B **109**: 7203

[3] Du X, Inokuchi M, Toshima N (2006) J Magnet Mater **299**: 21

[4] Vondrova M, Klimczuk T, Miller VL, Kirby BW, Yao N, Cava RJ, Bocarsly AB (2005) Chem Mater **17**: 6216

[5] Two selected examples : (a) Wan S, Huang J, Yan H, Liu K (2006) J Mater Chem **16**: 298; (b) Thünemann AF, Schütt D, Pison U, Möhwald H (2006) Langmuir **22**: 2351

[6] See i.e.: Sonvico F, Mornet S, Vasseur S, Dubernet C, Jaillard D, Degrouard J, Hoebeke J, Duguet E, Colombo P, Couvreur P (2005) Bioconjugate Chem **16**: 1181 and references cited therein

[7] Haddad PS, Duarte EL, Baptista MS, Goya GF, Leite CAP, Itri R (2004) Progr Coll Polym Sci **128**: 232

[8] Harris TJ, Maltzahn G, Derfus AM, Ruslahti E, Bhatia SN (2006) Angew Chem Int Ed **45**: 3161

[9] (a) Haryono A, Binder WH (2006) Small **2**: 600; (b) Farnik D, Kluger C, Kunz MJ, Machl D, Petraru L, Binder WH (2004) Macromol Sympos **217**: 247; (c) Binder WH (2005) Angew Chem Int Ed (2005) 5172; (d) Binder WH (2005) Monatsh Chemie 19

[10] (a) Binder WH, Petraru L, Roth T, Groh PW, Palfi V, Keki S, Ivan B (2007) Adv Funct Mater ASAP; (b) Binder WH, Bernstorff S, Kluger C, Petraru L, Kunz MJ (2005) Adv Mater **17**: 2824; (c) Binder WH, Kunz MJ, Ingolic E (2004) J Polym Sci Polym Chem **42**: 162; (d) Kunz MJ, Hayn G, Saf R, Binder WH (2004) J Polym Sci Polym Chem **42**: 661; (e) Petraru L, Farnik D, Saf R, Binder WH (2004) Polym Prepr **45**(2): 690

[11] Zirbs R, Kienberger F, Hinterdorfer P, Binder WH (2005) Langmuir **21**: 8414; (b) Binder WH, Kluger C, Straif CJ, Friedbacher G (2005) Macromolecules **38**: 9405; (c) Binder WH, Kluger C, Josipovic M, Straif CJ, Friedbacher G (2006) Macromolecules **39**: 8092; (d) Binder WH, Kluger C (2004) Macromolecules 9321

[12] Binder WH, Sachsenhofer R (2007) Macromol Rapid Commun **28**: 15

[13] Rockenberger J, Scher EC, Alivisatos AP (1999) J Am Chem Soc **121**: 11595

[14] Hyeon T, Lee SS, Park J, Chung Y, Na HB (2001) J Am Chem Soc **123**: 12798

[15] Webmineral, http://www.webmineral.com/data/Maghemite.shtml, 2006, Vol. 2006

[16] Crispino GA, Ho PT, Sharpless KB (1993) Science **259**: 64

[17] Boal AK, Das K, Gray M, Rotello VM (2002) Chem Mater **14**: 2628